ACS APPLIED MATERIALS & INTERFACES

Research Article

www.acsami.org

New Design Strategy for Reversible Plasticity Shape Memory Polymers with Deformable Glassy Aggregates

Tengfei Lin, Zhenghai Tang, and Baochun Guo*

Department of Polymer Materials and Engineering, South China University of Technology, Guangzhou, 510640, P. R. China

Supporting Information

ABSTRACT: Reversible plasticity shape memory (RPSM) is a new concept in the study of shape memory performance behavior and describes a phenomenon in which shape memory polymers (SMPs) can undergo a large plastic deformation at room temperature and subsequently recover their original shape upon heating. To date, RPSM behavior has been demonstrated in only a few polymers. In the present study, we implement a new design strategy, in which deformable glassy hindered phenol (AO-80) aggregates are incorporated into an amorphous network of epoxidized natural rubber (ENR) cured with zinc diacrylate (ZDA), in order to achieve RPSM properties. We propose that AO-80 continuously tunes the glass transition temperature (T_g) and improves the chain mobility of the SMP, providing traction and anchoring the ENR chains by intermolecular hydrogen bonding interactions. The RPSM behavior of the amorphous SMPs is characterized, and the results demonstrate good fixity at large deformations (up to 300%) and excellent recovery upon heating. Large energy storage capacities at T_d in these RPSM materials are demonstrated compared with those achieved at elevated temperature in traditional SMPs. Interestingly, the further revealed self-healing properties of these materials are closely related to their RPSM behavior.

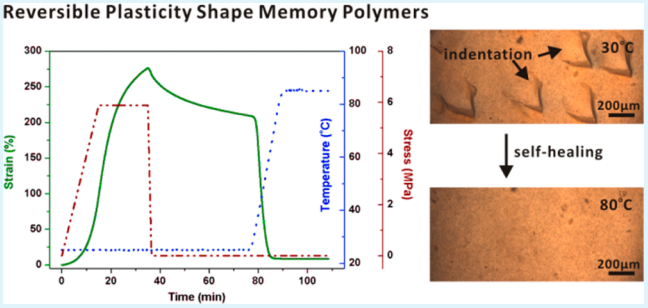

KEYWORDS: *shape memory polymers, reversible plasticity, amorphous network, self-healing*

INTRODUCTION

Shape memory polymers (SMPs) are a type of smart material. SMPs can be deformed into one or more temporary shapes and subsequently recover to their permanent shape when treated with appropriate stimuli, such as heat, light, and electricity.[1−5] Thermally induced SMPs are the most widely investigated of these materials.[6−8] Traditionally, thermally induced SMPs must be heated to a high temperature before deformation. The deformed SMPs are then cooled down under fixed stress to "freeze" the deformed polymer chains, thus achieving temporary shapes. Upon reheating, the polymer chains become mobile, and the material can relax by reverting to its original permanent shape.[9] This deforming and fixing process is not favorable because the heating and cooling steps require additional time and energy before and after deformation. Furthermore, heated SMPs in their rubbery state can only store a limited amount of energy. These issues raise the question of whether the fixing process can be simplified. Few SMP studies have addressed this, since most focus on studying complicated shape memory effects or tunable shape memory performance.

A novel shape memory assisted self-healing (SMASH) material, elegantly designed by Mather et al., provides a possible solution to simplify the fixing process.[10] The material can undergo a large plastic deformation at room temperature and recover upon heating, thus recovering both the temporal elastic and plastic regions of deformation. This novel phenomenon was termed reversible plasticity shape memory (RPSM)[10] or cold-drawing.[11] The RPSM concept has been used to prepared SMPs or self-healing polymers in several other studies.[12−14] This RPSM effect has been reviewed and regarded as "uniquely important" for SMPs.[15−17] The benefits of the RPSM effect include a simplified shape fixing process, potentially higher recovery stress, enhanced material deformability, and self-healing capacity.[16] Such properties are unusual and have been demonstrated for semicrystalline polymers to date.[14,18−20] During the deformation of a semicrystalline polymer, RPSM properties are thought to arise from the deformation of the crystalline lamellae and constituent polymer chains with an alignment parallel to the loading axis, such that they experience cold draw beyond the yield point. This PRSM mechanism for semicrystalline polymers is similar to "pseudo-plastic fixing" of shape memory alloys (SMAs), which occurs through a martensitic detwinning mechanism. Through this mechanism, the temporary shape of the SMAs is fixed at a constant temperature while recovery is triggered by heating above the martensitic−austenite phase transformation temperature.[9] As many polymer materials are amorphous and cross-linking tends to restrict the crystallization of polymers, it would be of great interest to design amorphous polymers with RPSM properties.

Received: September 1, 2014
Accepted: November 12, 2014
Published: November 12, 2014

Scheme 1. Chemical Structure of Hindered Phenol, AO-80

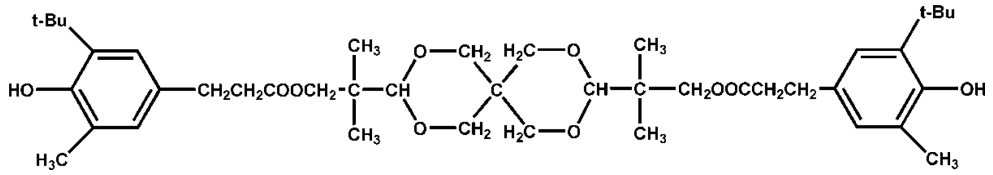

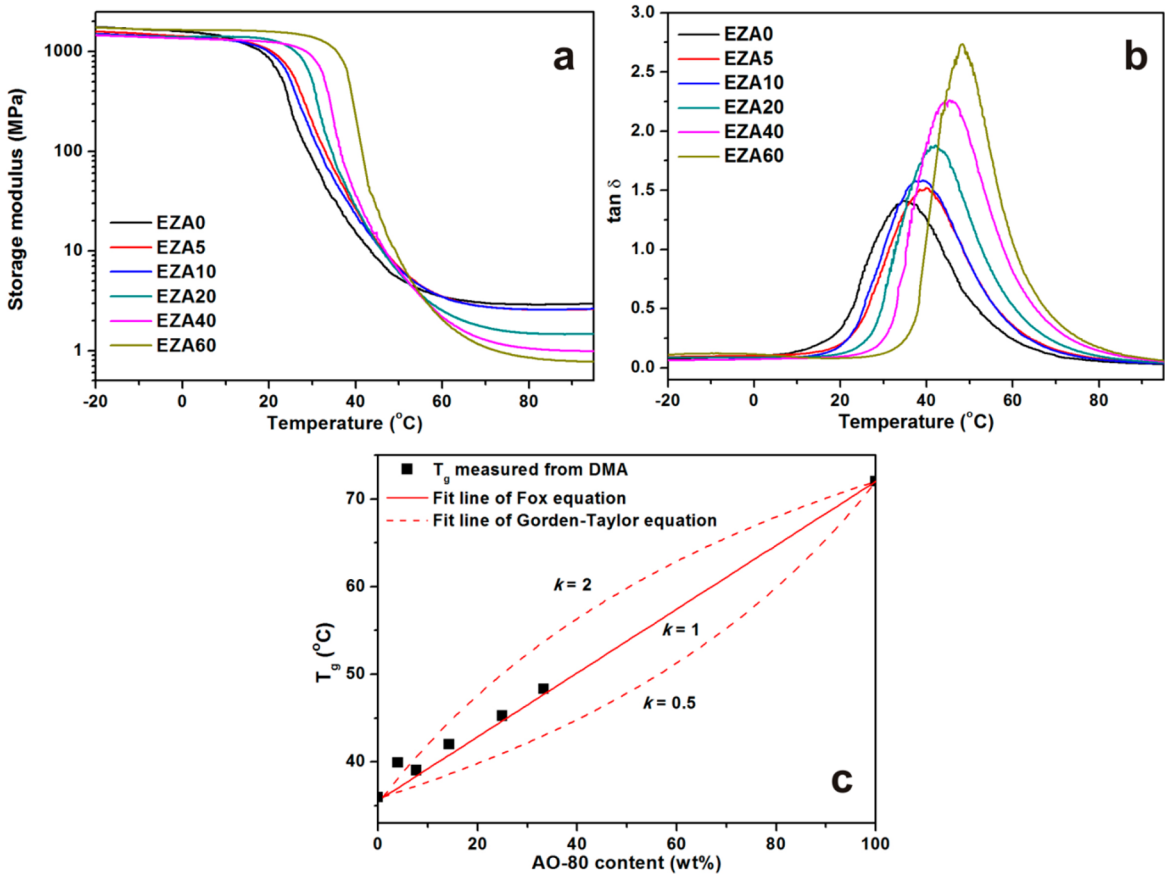

Figure 1. (a) Storage modulus (E'), (b) tan δ of EZA composites, and (c) T_g-composition behavior of the blends: solid points represent T_g measured by DMA, solid line represents curve-fitting based on the Fox equation, and dashed line represents curve-fitting based on the Gorden–Taylor equation. The T_g value (~72 °C) of AO-80 was sourced from the literature.[27]

In this study, we report a new design strategy for fabricating an amorphous polymer with RPSM features. Our strategy was to introduce AO-80, a hindered phenol of 3,9-bis[1,1-dimethyl-2-{*b*-(3-tertbutyl-4-hydroxy-5-methylphenyl)propionyloxy}-ethyl]-2,4,8,10-tetraoxaspiro-[5,5]-undecane (chemical structure is shown in Scheme 1), into an amorphous network of epoxidized natural rubber (ENR) cured by zinc diacrylate (ZDA). AO-80 is an additive that is generally used as antioxidant for polymers. It has also been reported that, through compounding with a polar polymer, AO-80 can acquire desirable features such as super damping and shape memorization.[21−24] In the present work, AO-80 is hypothesized to continuously tune the glass transition temperature (T_g) and improve the chain mobility of the ENR network, providing traction and anchoring the ENR chains by intermolecular hydrogen bonding interactions. This study describes the design of novel amorphous SMPs with RPSM behavior and characterizes the self-healing properties of these materials.

EXPERIMENTAL METHODS

Preparation of ZDA-Cured ENR/AO-80 Composites. ENR with an epoxidation degree of 50% was produced by the Agricultural Products Processing Research Institute, Chinese Academy of Tropical Agricultural Science, Zhanjiang, P. R. China. ZDA (zinc diacrylate, technically pure) was produced by the Xi'an Organic Chemical Factory, Xi'an, P. R. China. AO-80 was provided by Asahi Denka Co., Ltd. (Tokyo, Japan). ZDA-cured ENR/AO-80 composites were prepared as previously reported.[25] Briefly, ENR with a fixed amount of ZDA was mixed with varying amounts of AO-80 using an open two-roll mill. The well-mixed compounds were press-cured into 1 mm-thick sheets at 160 °C for 30 min. The sample name EZA-χ denotes a compound with χ parts AO-80 (relative to 100 parts ENR). All compounds were cured with 20 phr of ZDA.

Measurements. Tensile, tear, and hardness tests of the vulcanizates were performed at 25 °C, following ISO 37-2005, ISO 34-2004, and ISO 7619-2004, respectively. Tensile tests at elevated temperature and analysis of dynamic mechanical (DMA) and shape memory properties were performed with a TA Q800 dynamic mechanical analyzer (USA). After equilibrating at target temperature for 10 min, samples were stretched at 0.5 N/min, until the strain/stress limit was reached. Tensile tests at elevated temperature were repeated at least

three times, to ensure reproducibility. DMA was carried out under tension conditions, at a frequency of 1 Hz. The scanning temperature ranged from −100 to 100 °C, with a heating rate of 5 °C/min.

Reversible plasticity shape memory (RPSM) capacity was examined using a three-step thermomechanical cycling method. Prior to deformation, 5.0 × 6.0 × 0.2 mm^3 samples were heated to a deformation temperature (T_d) below the T_g and equilibrated for 10 min. In step 1, samples were deformed by applying a progressively increasing force, from a preloaded strain (ε_i) to a designated value with a strain of ∼300% (ε_m), at a rate of 0.5 N/min (deformation). The samples were held at ∼300% for 20 min to allow stress relaxation, yielding a strain of ε_m. In step 2, the force exerted on the samples was unloaded to the preloaded value of 0.005 N, at a rate of 0.5 N/min, after which a large percentage of plastic strain/deformation remained (ε_u) for all the tested samples. This was followed by an additional 40 min isothermal step to ensure shape fixing at a T_d below the T_g (unloading and shape fixing). In the final step, samples were reheated at a rate of 5 °C/min to 85 °C above T_g and held there for 20 min to a recovered strain, ε_r (recovery). The fixing (R_f) and recovery (R_r) ratios were calculated for each composition.

The R_f and R_r were defined as

$$R_f(\%) = \frac{\varepsilon_u - \varepsilon_i}{\varepsilon_m - \varepsilon_i} \times 100 \qquad R_r(\%) = \frac{\varepsilon_u - \varepsilon_r}{\varepsilon_u - \varepsilon_i} \times 100$$

Fourier transform infrared spectroscopy (FTIR) was performed on a Bruker Vertex 70 FTIR spectrometer with the samples in KBr pellets. X-ray diffraction (XRD) data were collected at ambient temperature on a Bruker D8 Advance X-ray diffractometer, using Cu Kα radiation (λ = 1.54 Å) with an accelerating voltage and current of 40 kV and 30 mA, respectively. Samples were scanned from 4° to 60°, with a step length of 0.02°, at 24 °C.

Cryogenically fractured sample surfaces were observed by scanning electron microscopy (SEM) with a Hitachi S-4800 FESEM (Japan). TEM observations for the ultramicrotomed samples were done by JEM-2010 machine (JEOL Ltd., Japan). A surface scratch test was performed with a hard metal indenter at room temperature. Samples were then heated to 80 °C and held at 80 °C for 5 min to allow for self-healing. The recovery process of the surface scratches was observed with an Olympus BX51 polarized light microscope (PLM).

RESULTS AND DISCUSSION

Previously, we reported a novel SMP based on natural rubber cross-linked via the oxa-Michael reaction.[25,26] We found that the SMP prepared with 20 phr ZDA possessed excellent shape fixity and shape recovery. In this study, ENR with 20 phr ZDA was compounded and cured with varying amounts of AO-80. These composites were assessed by dynamic mechanical analysis. Figure 1a,b shows the storage modulus and tan δ as a function of temperature. A single tan δ peak associated with the glass transition was observed for all samples. AO-80 particles showed good compatibility with ENR matrix and did not form a separated phase. Generally, various applications require SMPs to have a suitable transition temperature. In the present work, T_g values of all the EZA composites were above room temperature. The T_g value increased from 36.9 to 48.3 °C as the AO-80 content increased from 0 to 60 phr. The increased T_g values may be ascribed to the confinement of the rubber chains by the strong hydrogen bonding interactions between the ENR matrix and AO-80.[27] The storage modulus of EZA composites decreased with increasing AO-80 content. The tan δ peak intensities of EZA composites consistently increased with increasing AO-80 content, suggesting a continuous increase in chain mobility. Typically, the modulus below the switching temperature (crystalline and/or glassy modulus, E'_c and/or E'_g) governs the strength of the SMP, while the modulus above the switching temperature (rubbery modulus, E'_r) determines the recovery rate.[28] According to a hypothesis by Kim et al., a large drop in the storage modulus around T_g is essential for a polymer to be used as an SMP.[29] A high elasticity ratio (E'_g/E'_r), preferably with a minimum difference of 2 orders of magnitude, allows easy shaping at $T > T_g$, and high resistance to deformation at $T < T_g$. In the present system, all the EZA composites possessed a high elasticity ratio, with differences greater than 2−3 orders of magnitude with increasing AO-80 content (Table S1, Supporting Information). The EZA composites could be applied as traditional SMPs.

There are two kinds of hydrogen bonding interactions in the EZA system: the intermolecular hydrogen bonding between ENR and AO-80 and the intermolecular hydrogen bonding among AO-80 molecules.[27] To evaluate the interaction between ENR and AO-80, the Fox equation[30] and Gorden−Taylor equation[31] were utilized. Generally, these equations are used to predict the glass transition temperature of binary blends for compatible systems.

The Gorden−Taylor and Fox equations are expressed as follows (eqs 1 and 2, respectively).

$$T_g = (w_1 T_{g1} + k w_2 T_{g2})/(w_1 + k w_2) \quad (1)$$

$$T_g = w_1 T_{g1} + w_2 T_{g2} \quad (2)$$

Here T_g is the glass transition temperature of the blend, and w_i is the weight fraction of component i. The k parameter has been proposed to be related to the strength of intermolecular interactions between the blend components. A k value greater than 1 suggests a strong interaction between the two components, while a k value less than 1 suggests a relatively weak interaction. The Gorden−Taylor equation can be expressed as the Fox equation when the k value equals 1, thus representing a completely compatible system.

Figure 1c shows the variation of T_g with AO-80 content of EZA composites, with the fit lines calculated based on the Gorden−Taylor and Fox equations. The fit lines are concave or convex when the k values are either less than or greater than 1. The fit line is straight line when the k value equals 1. The DMA data show clearly that the measured T_g values correspond to the fit line for the Fox equation. The calculated k value is approximately equal to 1, indicating that the strength of the intermolecular hydrogen bonds between ENR and AO-80 equals that among AO-80 molecules. When AO-80 is added into the ENR, the intermolecular bonds between the hydroxyl and π-electrons of the benzene rings of AO-80[32] could be fully replaced by the intermolecular hydroxyl-oxirane ring bonds. The EZA composites therefore can be regarded as a completely compatible system. The chain mobility of the ENR network is largely improved with the addition of AO-80. Additionally, the T_g values of EZA composites with different AO-80 content can be predicted according to the Fox equation.

As a completely compatible system, AO-80 is expected to be homogeneously dispersed in the ENR matrix. Figure S2 (Supporting Information) shows SEM images of the cryogenically fractured surfaces of samples EZA40 and EZA60. The SEM images showed that the AO-80 particles were barely visible even at high magnification, thus indicating that, even at high concentrations, AO-80 particles were well-dispersed in the ENR matrix. To further study the microstructure of EZA composites, TEM observations are conducted. As shown in Figure 2, ZDA is not completely consumed during the curing process. The excessive ZDA generates nanoparticles with diameter about 20−100 nm. With the incorporation of AO-

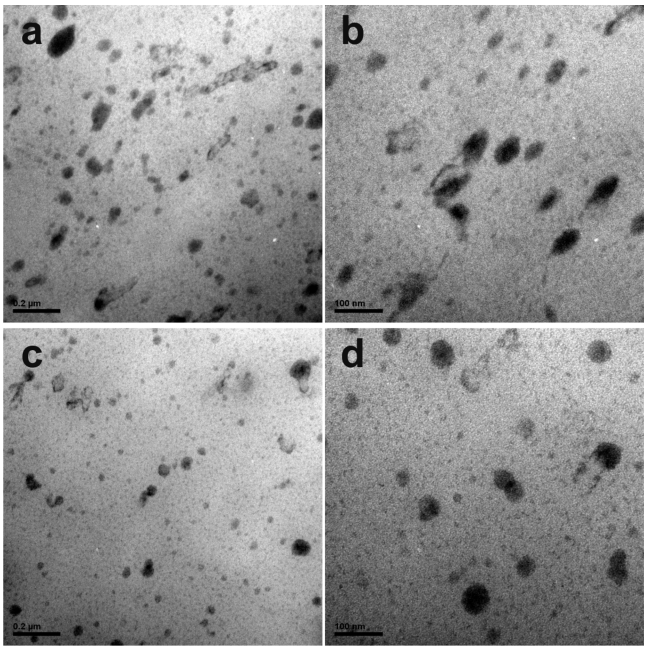

Figure 2. TEM photos of (a, b) EZA0 composites, (c, d) EZA40, respectively.

80, one can find the size of ZDA particles become much smaller (about 20−60 nm). AO-80 particles with diameter of 10 nm are found to be well-dispersed in the ENR matrix. It is believed that the fine dispersion of AO-80 particles in the polar ENR matrix results from mechanical shearing during the compounding process and from intermolecular hydrogen bonding between ENR and AO-80. A similar conclusion was reached in an earlier report on ENR/AO-80-based damping blends.[23] The finely dispersed AO-80 particles improve the chain mobility of ENR by decreasing the interchain interaction. Therefore, the incorporated AO-80 enables large plastic deformation below T_g.

Wide angle XRD (WAXD) patterns of EZA composites are shown in Figure S3 (Supporting Information). These have revealed that most hindered phenol substances can be crystalline or amorphous, depending upon the processing conditions.[32,33] Nanoscaled amorphous AO-80 particles can be generated by mechanically kneading AO-80 with a polar rubber such as nitrile butadiene rubber (NBR), followed by vulcanization at a temperature higher than the melting point of AO-80 (122.5 °C).[23] In the present work, the well-mixed compounds were press-cured at 160 °C for 30 min. As expected, only a broad diffuse peak is observed for EZA composites with AO-80, since they are completely compatible blends. For EZA0 (which does not contain AO-80), a peak was observed at 6.40°, which is the result of the formation of tiny crystallites of poly(acrylic acid).[25,34] The addition of AO-80 resulted in the disappearance of the diffraction peak at ∼6.40°, suggesting restricted formation of the crystallites. EZA composites with AO-80 were confirmed to be completely amorphous polymers.

Figure 3 depicts the effect of AO-80 content on the mechanical properties of EZA composites at 25 °C and at 40 °C above the T_g. Figure 3a shows the effect of AO-80 loading on the tensile properties of ENR at room temperature (data summarized in Supporting Information Table S1). All the EZA composites possessed a tensile strength above 20 MPa. As a low molecular weight additive, AO-80 is not expected as an effective reinforcing agent for ENR, although it has been demonstrated to be effective in reinforcing nitrile rubber.[23] The addition of AO-80 (except at 60 phr) exhibited an insignificant effect on the tensile strength and elongation of EZA composites. When the AO-80 content was lower than 20 phr, the cross-linked ENR composites behaved like soft rubber. When the AO-80 content was higher than 20 phr, the composites behaved like rigid plastics, exhibiting definite yielding. Such yielding behavior is more apparent with higher AO-80 content. Additionally, the modulus and tear strength of all EZA composites significantly increased with increasing AO-80 content. These observations also imply a continuously increasing T_g. At a temperature above T_g, tensile strength decreases significantly, as shown in Figure 2b. At this elevated temperature, EZA composites with high AO-80 content did not exhibit yielding behavior, suggesting that they transformed into an elastomer. The elongation length at the breaking point increased with increasing AO-80 content at the elevated temperature. This may be due to the intermolecular hydrogen bonds causing the ENR molecules to slide with the AO-80 molecules along the strectching direction, thus orienting the ENR chains along the loading axis and resulting in an increasing elongation length at the breaking piont.

The progression of RPSM behavior for the sample EZA40 is shown in Figure 4 (videos S6 and S7 in the Supporting Information). In Figure 4a, the initial sample was stretched to

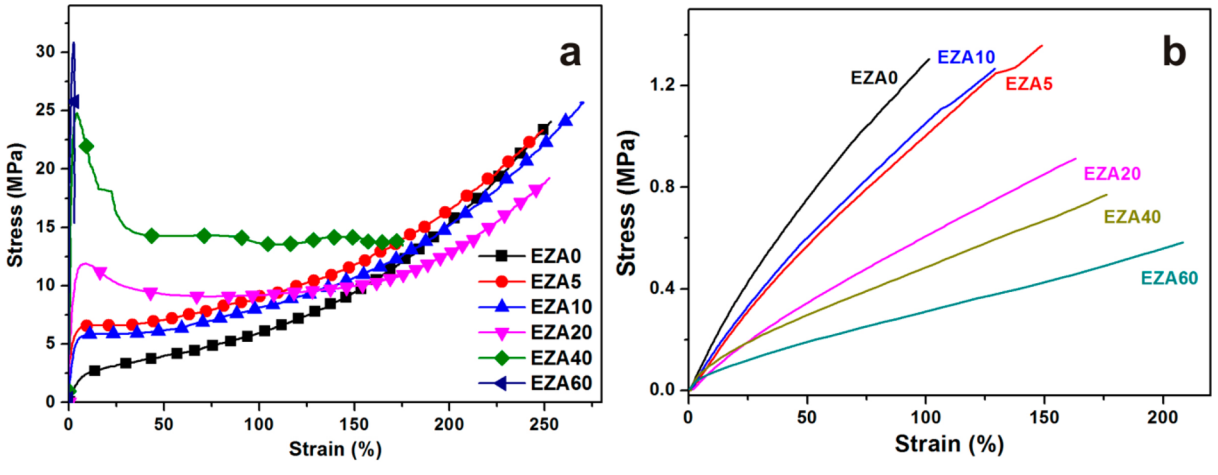

Figure 3. Tensile stress−strain curves of EZA composites at (a) room temperature (25 °C) and (b) elevated temperature (40 °C above the T_g).

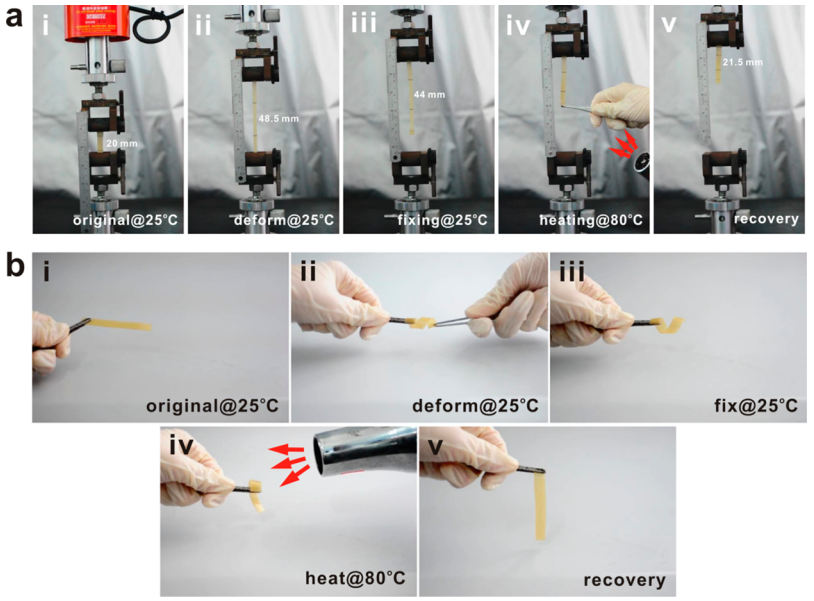

Figure 4. Sample EZA40, whose permanent shape is a stripe, exhibits RPSM behavior. (a) The sample was stretched at a crosshead speed of 30 mm/min and fixed to achieve temporary deformation. (b) The sample was nonaxial deformed and fixed to achieve a temporary spiral shape. The stretching/deforming and fixing processes were performed at a constant temperature (25 °C). The samples then recovered to their permanent shape after heating to 80 °C (videos in the Supporting Information).

achieve ~140% strain at a constant temperature (25 °C). The strain was maintained after releasing the lower clamp holding the sample. For traditional plastic polymers, such deformation is considered irreversible and is called "permanent deformation". However, in the present system, the deformation is unusual in its reversible nature. The deformed EZA40 sample recovered to its initial length upon heating to 80 °C. Furthermore, EZA40 was able to demonstrate RPSM behavior even under nonaxial deformation, such as spiral deformation (Figure 4b). A temporary spiral shape was created by plastic deformation at room temperature and was maintained even after the load was released. Upon heating, the original shape was recovered rapidly. These experiments demonstrate that EZA40 exhibits good RPSM performance.

For most traditional SMPs, the trigger temperature is usually over only a narrow temperature range. Therefore, the deformations were usually limited, which may significantly limit its application.[10,18,20] In the present work, the amorphous SMPs were demonstrated to achieve large plastic deformation. The selection of deformation temperature (T_d) for the RPSM cycle is important. In their glassy state, polymer chains are "frozen" and fragile at low temperatures. Heating may cause glassy polymers to transition into a rubbery state, in which the polymer chains become elastic and no longer undergo plastic deformation. Therefore, the T_d must be carefully chosen to be near the onset of the glass transition in order for amorphous SMPs to achieve large plastic deformation. With a benefit from the broader T_g range of 50−60 °C, large plastic deformation of EZA composites can be achieved (data summarized in Table 1),

Table 1. Shape Memory Characteristics of EZA Composites

samples	T_d (°C)	ε_{load} (%)	ε_f (%)	ε_r (%)	R_f (%)	R_r (%)
EZA0	15	330.5	238.3	78.1	72.1	67.3
EZA20	23	303.2	214.3	40.9	70.7	80.9
EZA40	25	276.4	209.1	8.4	75.6	96.0
EZA60	27	312.2	227.6	39.7	72.9	82.6

as the chain mobility of EZA composites is significantly improved with the addition of AO-80. In other words, AO-80 particles could be regarded as "plasticizer" in EZA composites since the interaction between ENR and AO-80 is comparable to that among AO-80 particles. Representative DMA data for EZA40 undergoing a RPSM cycle is shown in Figure 5a. During the deformation step, EZA40 was stretched at 25 °C to ~300% strain to achieve temporary deformation. The stress was released to observe the initial elastic shape recovery for over 40 min. The deformed sample was then heated to 85 °C to trigger the shape recovery. Other EZA composites with variable AO-80 content were tested in a similar manner and were found to exhibt similar RPSM behavior as EZA40 (Figure S4, Supporting Information). Shape memory fixing and recovery ratios, R_f and R_r, were calculated for the EZA samples and are presented in Table 1. All composites achieved a temporary deformation of ~300% strain before unloading (ε_m) and a strain ranging from 209.1% to 238.3% after unloading (ε_u). The residual strain after shape recovery could be ascribed to the rearrangement of polymer molecule chains and AO-80 aggregates. The residual strain was quite small compared to the high temporary deformation (~300%) that each sample achieved prior to shape recovery. R_f, which ranged from 70.7% to 75.6%, was independent of AO-80 concentration. R_f values of the amorphous EZA composites were slightly lower than that of a previously studied semicrystalline polymer (as high as 80.9%).[10] This difference may be attributed to the fact that the mechanism for RPSM behavior in amorphous polymer is thermodynamically unstable compared with the rearrangement of crystalline lamellae in semicrystalline polymers, although R_f values for RPSM may not be comparable with those for conventional SM condition. The importance of RPSM may not lie in the shape fixing, but in the simplified shape fixing process, potentially higher recovery stress, enhanced material deformability, and self-healing, as summarized by Xie.[16] Actually, considering the very high deformation (300%), the present fixity ranging from 70.7% to 75.6% is remarkably high. Also

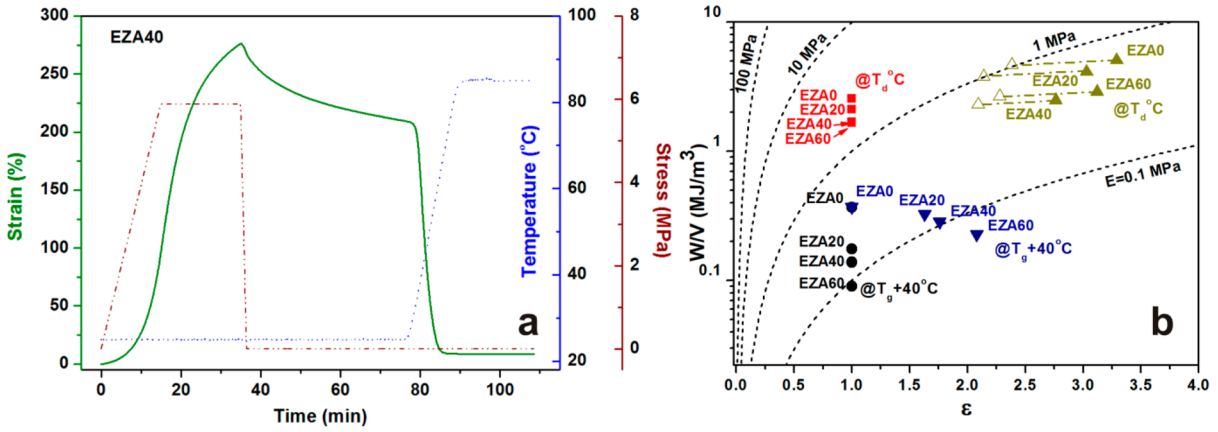

Figure 5. (a) Reversible plasticity shape memory (RPSM) cycle of the composite EZA40. The sample was stretched to a strain of ~300% at 25 °C and was allowed to recover at 85 °C. Strain vs time (green, solid), stress vs time (red, dashed), and temperature vs time (blue, dotted) curves are shown. (b) Deformation/stored energy densities for EZA composites at different stress−strain conditions. Filled black circles and filled red squares represent the deformation energy density of EZA samples when stretched to a strain of 100% at elevated temperature (40 °C above the T_g) and at T_d, respectively. Filled blue lower triangles and dark yellow upper triangles represent the maximum value of deformation energy densities for EZA composites at elevated temperature and at T_d, respectively. Hollow triangles represent the stored energy density following load removal. Dashed lines are reference lines that show the elastic behavior of ideal neo-Hookean solids.

such deformation could be fixed over long-standing time (over 40 min). Unlike R_f, the R_r value increased from 67.3% to 96.0% with increasing AO-80 up to 40 phr. However, at higher AO-80 content (60 phr), R_r decreased to 82.6%. As mentioned above, the irrecoverable deformation may be due to the rearrangement of polymer chains and AO-80 aggregates. With increased incorporation of AO-80, increasing amounts of AO-80 fine aggregates are created, which increases the interaction between AO-80 and the polymer chains. Therefore, R_r increases with increasing AO-80 content. However, when excessive AO-80 is used, AO-80 may aggregate into larger particles which increases the risk of rearrangement during the recovery stage. Therefore, incorporation of excessive AO-80 lowers R_r. The composite EZA0, which does not have any AO-80, showed the RPSM to some extent. As the T_g range of EZA0 is much broader (~60 °C) compared to traditional SMPs, it exhibits the RPSM behavior since some parts of the polymer chain are still mobile when below the T_g. Nevertheless, EZA0 composite showed the poorest shape recovery, which may be due to its limited chain mobility, as evidenced by DMA results (Figure 1). Altogether, these results show that RPSM behavior can be achieved in an amorphous cross-linked polymer system.

According to the model proposed by Anthamatten et al., the energy storage capacity of SMPs can be quantified from their stress−strain (σ, ε) relationship.[35] SMPs were assumed as incompressible, isotropic neo-Hookean solids.[36,37] Thus, the neo-Hookean relationship between stress and strain is expressed as follows.

$$\sigma = G\left[(1+\varepsilon)^2 - \frac{1}{(1+\varepsilon)}\right] \quad (3)$$

Here G is the shear modulus and can be obtained from a single stress−strain point. The elastic work density required to deform a sample to an elongation ε is

$$\frac{W}{V} = G\left[\frac{(1+\varepsilon)^2}{2} + \frac{1}{(1+\varepsilon)} - \frac{3}{2}\right] \quad (4)$$

where V is the sample volume. This work energy density represents an upper bound of elastic energy that can be stored in an SMP upon elastic deformation. Although the calculated energy densities were only estimated values, the use of the neo-Hookean model may be appropriate here since only a single point from the stress−strain curve is required.[35] Hence, the energy densities of EZA series could be roughly estimated and compared.

Figure 5b shows the calculated deformation/stored energy densities for EZA composites at different stress−strain conditions. Compared with those at elevated temperature above T_g, the energy storage capacities for SMPs with RPSM behavior at T_d increase significantly. When stretched to 100% strain, the deformation energy densities for EZA composites at T_d are much higher than those at elevated temperature (40 °C above T_g). For example, the deformation energy density for sample EZA40 is 1.68 MJ/m^3 at T_d, which is more than 10-fold higher than that achieved at elevated temperature. The deformation energy density increases with increasing elongation. At elevated temperature, the maximum values of deformation energy densities for EZA composites ranged from 0.37 to 0.23 MJ/m^3 with increasing AO-80 content. These results are consistent with the estimated elastic energy densities for most of the literature data (between 0.01 to 1.5 MJ/m^3).[35] However, at T_d, the maximum values of deformation energy densities for RPSM cycles of EZA composites increase significantly, ranging from 5.07 to 2.88 MJ/m^3. These represent 11−12-fold increases compared with those at elevated temperature. The stored energy densities after unloading decreased slightly, which is attributed to the partial recovery of deformation. With such high stored energy densities, SMPs could be more useful for possessing high recovery stress upon heating, such as intelligent and powerful gripper.

RPSM behavior may assist in the self-healing process by facilitating crack closure or by healing nonpermanent defects. Several studies have shown that RPSM performance can improve the ability of polymer to heal from nonpermanent surface defects (e.g., indents or scratches) upon thermal activation.[12,14,38] To evaluate this, we therefore employed scratch/indentation tests using the EZA composite samples at room temperature. The results of the scratch tests are shown in Figure 6. In the scratch tests, an indenter with a pyramidal

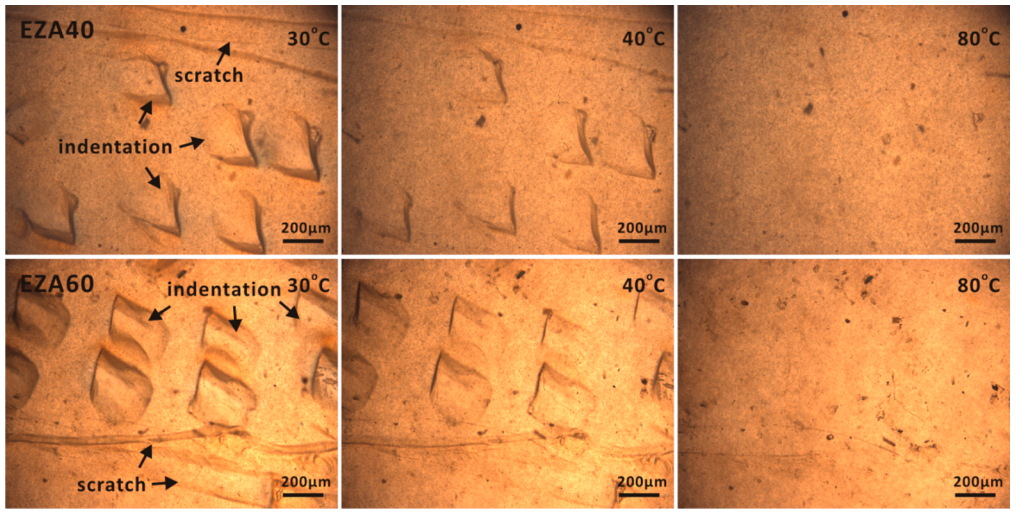

Figure 6. Optical images of the surfaces of samples EZA40 and EZA60, depicting the self-healing after scratch/indentation test.

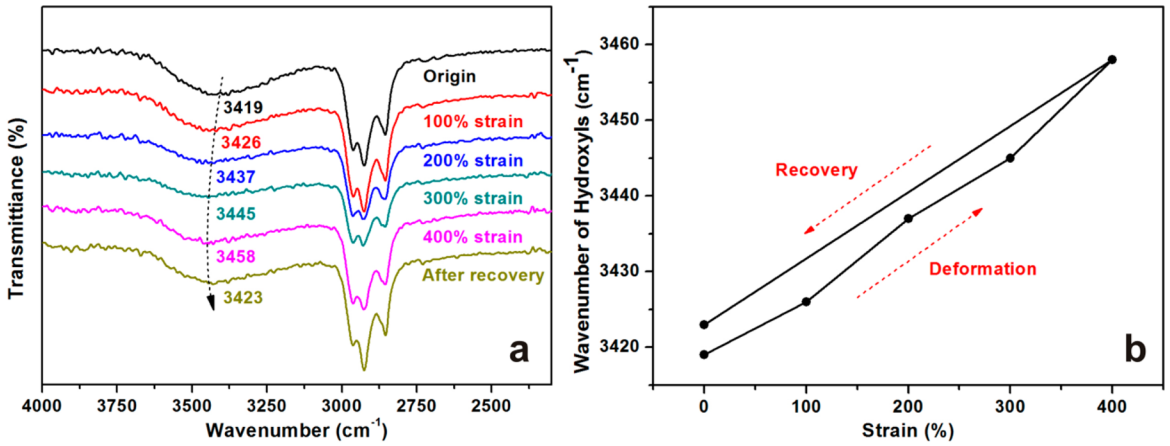

Figure 7. (a) FTIR spectra of the stretched EZA40 composite at different strain conditions and (b) the dependence of the hydroxyl band on strain.

shape was inserted at a slanted angle into the material or moved horizontally across the material surface under a constant load to create indentations or scratches, respectively (Figure 6, arrows). As the EZA composites were gradually heated to 80 °C under stress-free conditions, the scratches and indentations were partially healed at 40 °C and were completely healed at 80 °C. These scratch/indentation tests therefore confirmed that RPSM behavior can assist in the self-healing of amorphous EZA composites.

In an effort to understand the mechanism for RPSM behavior in EZA composites, we obtained FTIR spectra of the composite EZA40 at different strain conditions, and we observed a dependence of the hydroxyl band on strain (Figure 7). In the FTIR spectrum of EZA40 prior to stretching, the absorption peak around 3419 cm^{-1} is assigned to hydroxyl stretching vibrations generated by the ring-opening of ENR and the addition of AO-80.[27] When the EZA40 sample was continuously stretched, many changes were observed in the infrared spectrum. Compared to the spectrum obtained prior to stretching, the hydroxyl absorption band of the stretched sample shifted to a higher wavenumber, from 3419 to 3458 cm^{-1}, with increasing strain. Other absorption peaks did not shift during stretching (Figure S5, Supporting Information). As discussed above, the calculated k value based on the Fox equation approximately equal to 1. Thus, the intermolecular hydrogen bonding between ENR and AO-80 is assumed to be equal to the intermolecular hydrogen bonds of AO-80, a condition that favors the miscibility of the two components. During the stretching process, the relative relationship or interfacial interaction between AO-80 and the ENR chains may change significantly with the motion of the molecules, thus altering the hydrogen bonding between AO-80 and the ENR chains and shifting the hydroxyl absorption. Interestingly, when the stretched sample recovers to its initial length after heating to above 80 °C, the hydroxyl absorption band shifts back to its initial value. The recovery of the initial hydroxyl band can be attributed to the recovery of the initial relative relationship between AO-80 and the ENR chains and the dissociation of the hydrogen bonds formed between them.

There are two essential requirements to achieve RPSM performance in an amorphous SMP. One requirement is that a given amorphous SMP must experience plastic-like deformation (i.e., yielding) under nonheated conditions. The deformation temperature must be near the onset of glass transition in order to achieve large plastic deformation in an amorphous SMP.[39] At the deformation temperature, some parts of the polymer chains become mobile while other parts are still "frozen", thus achieving large plastic deformation. The deformation is at least partially retained after removal of the stress (shape fixation). The second requirement is that the given amorphous SMP

Scheme 2. Molecular RPSM Mechanism for EZA Composite: (a) Permanent State and (b) Temporary State

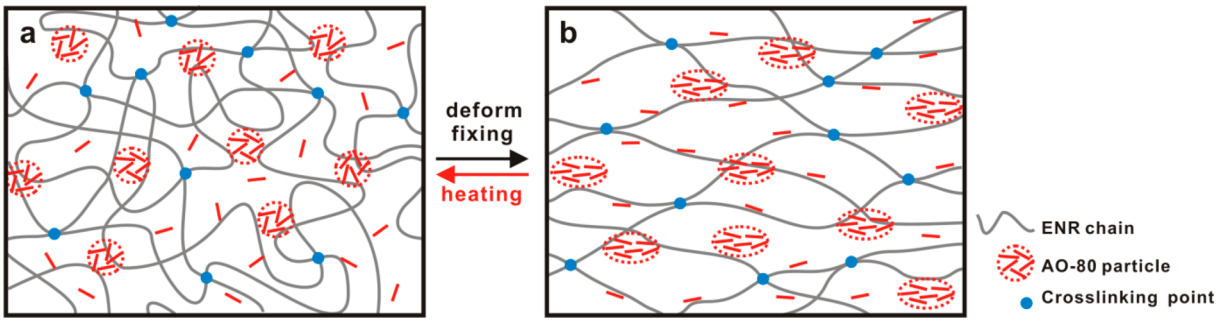

must have enough entropy elasticity for the shape recovery upon heating. Cross-linking is the most practical way to achieve entropy elasticity, and to endow the deformed SMP with reversibility properties. On the basis of the above discussion, we propose a mechanism for RPSM behavior in amorphous EZA composites (schematically shown in Scheme 2). The cross-linked ENR chains are initially randomly arranged and tangled under a stress-free condition. The compatible, low molecular weight additive AO-80 is added and dispersed uniformly in ENR matrix, which increases the chain mobility of the ENR network. During the stretching process, AO-80 particles slide along the loading axis, and the intermolecular hydrogen bonding between AO-80 and ENR causes the ENR chains to tighten and align during the tensile deformation. The large plastic deformation is maintained after the removal of stress because the tense ENR chains are trapped due to their glassy status and their anchoring to the deformed AO-80 particles. Upon heating to a temperature above T_g, the AO-80 particles melt, and the EZA composites gradually transition from a glassy state to a rubbery state. The ENR chains become elastic with decreased hydrogen bonding between the ENR and AO-80. Driven by the entropy elasticity, the tense cross-linked network shrinks and recovers its initial randomly arranged and tangled status. AO-80 is also thermodynamically rearranged into its initial aggregate formation.

CONCLUSION

This study presents a new design strategy for RPSMPs with deformable glassy aggregates. We created composite materials by incorporating compatible, low molecular weight AO-80 into an ENR network cross-linked by ZDA. SMPs with RPSM behavior could simplify the shape fixing process, saving additional time and energy. These composite materials could undergo a large plastic deformation of ~300% strain that was achieved at a T_d that was below T_g and maintained when the stress was released. Large energy storage capacities at T_d in these RPSM materials were demonstrated compared with those achieved at elevated temperature in traditional SMPs. Upon heating to a temperature above T_g, the materials recovered their original shape almost completely. Therefore, such SMPs could be useful for possessing high recovery stress, such as intelligent and powerful gripper. Self-healing tests showed that non-permanent damages of the amorphous EZA composites were well-healed when the samples were heated to a temperature above T_g. We propose a potential mechanism for RPSM behavior of EZA composites. We anticipate that incorporation of compatible, low molecular weight additives into an amorphous network could be a universal method for fabricating amorphous SMPs with RPSM behavior. We also hypothesize that the prerequisites for RPSM behavior of amorphous polymers have excellent compatibility between the additive and the network and the formation of fine deformable glassy aggregates.

ASSOCIATED CONTENT

Supporting Information

Mechanical data (Table S1), SEM images (Figure S2), WAXD patterns (Figure S3). Reversible plasticity shape memory cycle for EZA0, EZA20, and EZA60 composites (Figure S4). FTIR spectra (Figure S5) and videos showing the RPSM performance (video S6, video S7). This material is available free of charge via the Internet at http://pubs.acs.org/.

AUTHOR INFORMATION

Corresponding Author

*E-mail: psbcguo@scut.edu.cn. Phone: +86 20 87113374. Fax: +86 20 22236688.

Notes

The authors declare no competing financial interest.

ACKNOWLEDGMENTS

The authors acknowledge financial support from the National Natural Science Foundation of China (Nos. 51222301, 51473050, and 51333003), Research Fund for the Doctoral Program of Higher Education of China (No. 20130172110001), and Fundamental Research Funds for the Central Universities (No. 2014ZG0001).

REFERENCES

(1) Lendlein, A.; Jiang, H.; Jünger, O.; Langer, R. Light-induced shape-memory polymers. *Nature* **2005**, *434*, 879−882.
(2) Gil, E. S.; Hudson, S. M. Stimuli-reponsive polymers and their bioconjugates. *Prog. Polym. Sci.* **2004**, *29*, 1173−1222.
(3) Huang, W.; Yang, B.; An, L.; Li, C.; Chan, Y. Water-driven programmable polyurethane shape memory polymer: Demonstration and mechanism. *Appl. Phys. Lett.* **2005**, *86*, 114105.
(4) Liu, Y.; Lv, H.; Lan, X.; Leng, J.; Du, S. Review of electro-active shape-memory polymer composite. *Compos. Sci. Technol.* **2009**, *69*, 2064−2068.
(5) Kumpfer, J. R.; Rowan, S. J. Thermo-, photo-, and chemo-responsive shape-memory properties from photo-cross-linked metallo-supramolecular polymers. *J. Am. Chem. Soc.* **2011**, *133*, 12866−12874.
(6) Behl, M.; Lendlein, A. Shape-memory polymers. *Mater. Today* **2007**, *10*, 20−28.
(7) Luo, Y. W.; Guo, Y. L.; Gao, X.; Li, B. G.; Xie, T. A general approach towards thermoplastic multishape-memory polymers via sequence structure design. *Adv. Mater.* **2013**, *25*, 743−748.
(8) Kratz, K.; Madbouly, S. A.; Wagermaier, W.; Lendlein, A. Temperature-memory polymer networks with crystallizable controlling units. *Adv. Mater.* **2011**, *23*, 4058−4062.

(9) Liu, C.; Qin, H.; Mather, P. Review of progress in shape-memory polymers. *J. Mater. Chem.* **2007**, *17*, 1543−1558.
(10) Rodriguez, E. D.; Luo, X.; Mather, P. T. Linear/network poly(ε-caprolactone) blends exhibiting shape memory assisted self-healing (SMASH). *ACS Appl. Mater. Interfaces* **2011**, *3*, 152−161.
(11) Lendlein, A.; Kelch, S. Shape-memory polymers. *Angew. Chem., Int. Ed.* **2002**, *41*, 2034−2057.
(12) Xiao, X.; Xie, T.; Cheng, Y. Self-healable graphene polymer composites. *J. Mater. Chem.* **2010**, *20*, 3508−3514.
(13) Koerner, H.; Price, G.; Pearce, N. A.; Alexander, M.; Vaia, R. A. Remotely actuated polymer nanocomposites—stress-recovery of carbon-nanotube-filled thermoplastic elastomers. *Nat. Mater.* **2004**, *3*, 115−120.
(14) Li, G.; Ajisafe, O.; Meng, H. Effect of strain hardening of shape memory polymer fibers on healing efficiency of thermosetting polymer composites. *Polymer* **2013**, *54*, 920−928.
(15) Xiao, R.; Choi, J.; Lakhera, N.; Yakacki, C. M.; Frick, C. P.; Nguyen, T. D. Modeling the glass transition of amorphous networks for shape-memory behavior. *J. Mech. Phys. Solids* **2013**, *61*, 1612−1635.
(16) Xie, T. Recent advances in polymer shape memory. *Polymer* **2011**, *52*, 4985−5000.
(17) Li, G.; Xu, W. Thermomechanical behavior of thermoset shape memory polymer programmed by cold-compression: Testing and constitutive modeling. *J. Mech. Phys. Solids* **2011**, *59*, 1231−1250.
(18) Meng, Q.; Hu, J.; Zhu, Y.; Lu, J.; Liu, Y. Polycaprolactone-based shape memory segmented polyurethane fiber. *J. Appl. Polym. Sci.* **2007**, *106*, 2515−2523.
(19) Ping, P.; Wang, W.; Chen, X.; Jing, X. Poly(ε-caprolactone) polyurethane and its shape-memory property. *Biomacromolecules* **2005**, *6*, 587−592.
(20) Mohr, R.; Kratz, K.; Weigel, T.; Lucka-Gabor, M.; Moneke, M.; Lendlein, A. Initiation of shape-memory effect by inductive heating of magnetic nanoparticles in thermoplastic polymers. *Proc. Natl. Acad. Sci. U.S.A.* **2006**, *103*, 3540−3545.
(21) Wu, C.; Yamagishi, T. A.; Nakamoto, Y.; Ishida, S.; Nitta, K. H.; Kubota, S. Organic hybrid of chlorinated polyethylene and hindered phenol. I. Dynamic mechanical properties. *J. Polym. Sci., Part B: Polm. Phys.* **2000**, *38*, 2285−2295.
(22) Wu, C.; Akiyama, S.; Mabuchi, T.; Nitta, K. H. Dynamic mechanical properties and morphologies of organic hybrids consisting of chlorinated polyethylene and hindered phenol. *Polym. J. (Tokyo, Jpn.)* **2001**, *33*, 792−798.
(23) Zhao, X.; Xiang, P.; Tian, M.; Fong, H.; Jin, R.; Zhang, L. Nitrile butadiene rubber/hindered phenol nanocomposites with improved strength and high damping performance. *Polymer* **2007**, *48*, 6056−6063.
(24) Zhao, X.; Lu, Y.; Xiao, D.; Wu, S.; Zhang, L. Thermoplastic ternary hybrids of polyurethane, hindered phenol and hindered amine with selective two-phase dispersion. *Macromol. Mater. Eng.* **2009**, *294*, 345−351.
(25) Lin, T.; Ma, S.; Lu, Y.; Guo, B. New design of shape memory polymers based on natural rubber crosslinked via oxa-Michael reaction. *ACS Appl. Mater. Interfaces* **2014**, *6*, 5695−5703.
(26) Lin, T.; Guo, B. Curing of rubber via oxa-Michael reaction toward significantly increased aging resistance. *Ind. Eng. Chem. Res.* **2013**, *52*, 18123−18130.
(27) Li, C.; Cao, D.; Guo, W.; Wu, C. The investigation of miscibility in blends of ENR/AO-80 by DMA and FT-IR. *J. Macromol. Sci., Part B: Phys.* **2007**, *47*, 87−97.
(28) Zhang, C.; Ni, Q. Bending behavior of shape memory polymer based laminates. *Compos. Struct.* **2007**, *78*, 153−161.
(29) Kim, B. K.; Lee, S. Y.; Xu, M. Polyurethanes having shape memory effects. *Polymer* **1996**, *37*, 5781−5793.
(30) Fox, T. G. Influence of diluent and of copolymer composition on the glass temperature of a polymer system. *Bull. Am. Phys. Soc.* **1956**, *1*, 123.
(31) Coleman, M. M.; Yang, X.; Painter, P. C.; Graf, J. F. Equilibrium constants and the prediction of phase behavior for phenoxy blends with aliphatic polyesters. *Macromolecules* **1992**, *25*, 4414−4424.
(32) Wu, C. Relaxation effects in an organic glassy material. *J. Non-Cryst. Solids* **2003**, *315*, 321−324.
(33) Lohmeijer, J. Polymer/additive compatibility: Study of primary antioxidants in PBD. *J. Appl. Polym. Sci.* **1997**, *65*, 761−775.
(34) Yu, Q.; Wang, X.; Shen, Y.; Tao, Y.; Xie, A. Preparing and physicochemical properties of microcrystalline polyacrylic acid gels. *Russ. J. Phys. Chem. A* **2013**, *87*, 2100−2104.
(35) Anthamatten, M.; Roddecha, S.; Li, J. Energy storage capacity of shape-memory polymers. *Macromolecules* **2013**, *46*, 4230−4234.
(36) Rivlin, R. Large elastic deformations of isotropic materials. IV. Further developments of the general theory. *Philos. Trans. R. Soc., A* **1948**, *241*, 379−397.
(37) Mooney, M. A theory of large elastic deformation. *J. Appl. Phys.* **1940**, *11*, 582−592.
(38) Wornyo, E.; Gall, K.; Yang, F.; King, W. Nanoindentation of shape memory polymer networks. *Polymer* **2007**, *48*, 3213−3225.
(39) Yakacki, C. M.; Willis, S.; Luders, C.; Gall, K. Deformation limits in shape-memory polymers. *Adv. Eng. Mater.* **2008**, *10*, 112−119.